METRO
MEtallurgical TRaining On-line

Computer modeling of phase transformation of cast alloys in solid state especially taking into consideration ADI castings

Lecture II: ADI, ausferrite growth

Wojciech Kapturkiewicz
AGH

Education and Culture

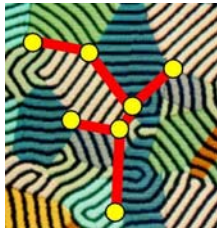

Ausferrite growth

Abstract of Lecture

A model of ausferrite growth in ADI was presented together with results from the simulation program. Their application enables tracing of the process of ausferrite growth, i.e. of the high-carbon ferrite in austenite. The model was based on a transient diffusion growth of ferrite lamellae in austenite under the boundary conditions proper for the austempering temperature and allowing for the function of ferrite nucleation. The results of the simulation were compared with the data obtained in experiments.

Kewords:

modelling, ausferrite, ADI

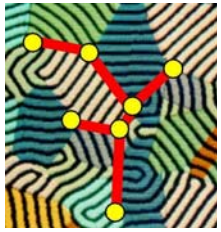

Ausferrite growth

Introduction

Cast iron is a material in which the transformation in solid phase can change in an essential way the primary structure, which in this case is only a starting point for further phase transformations. The subject of this study is ductile iron subjected to further heat treatment typical of **ADI** (**A**ustempered **D**uctile **I**ron).

In the ductile iron in solid state the following phase transformations of austenite are of special importance:

- austenite – ferrite or/and pearlite during cooling of ductile iron in a foundry mould,
- austenite – ferrite in ADI technology.

Rapid cooling of casting (Fig. 1) from austenitizing (820 - 950^{0}C to austempering temperature (240 – 400^{o}C) changes the conditions of equilibrium, resulting in nucleation and growth of ferrite in austenite. A typical structure with acicular ferrite and austenite is called ausferrite.

The structure most desired in ADI is high-carbon ferrite in a matrix of reacted high-carbon austenite (i.e. ausferrite) with graphite nodules typical of ductile iron.

Ausferrite growth

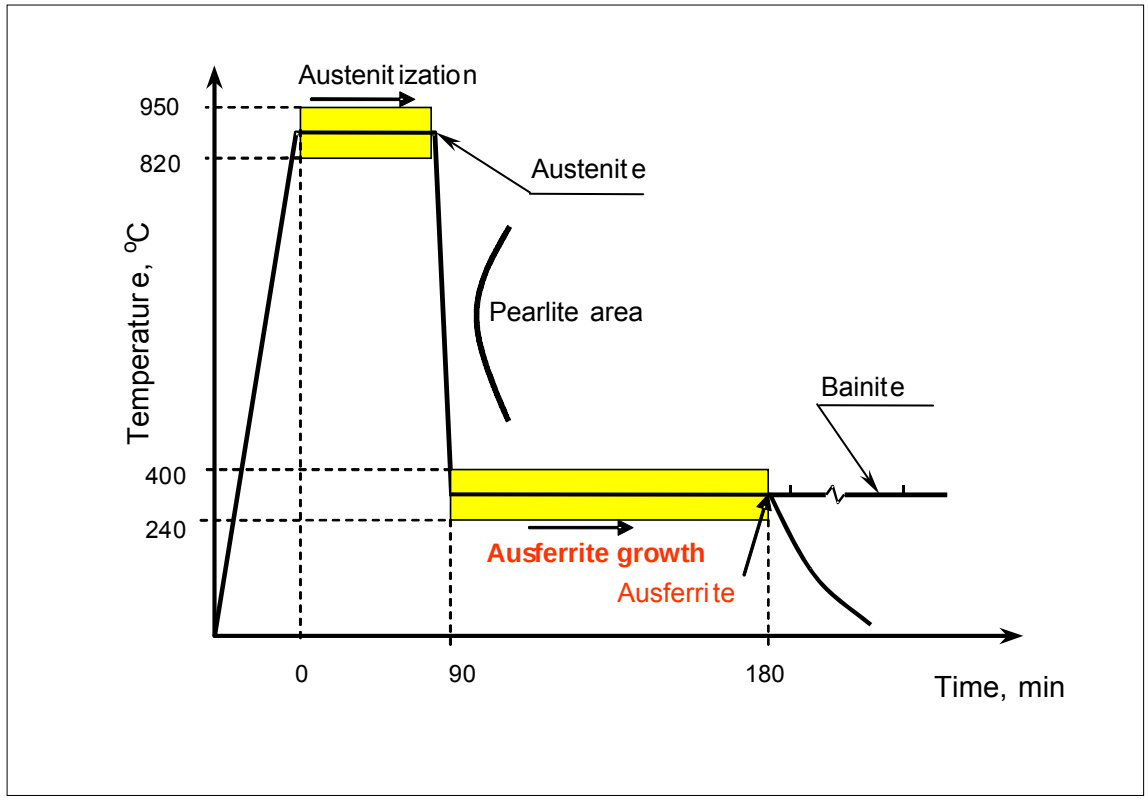

Fig. 1. Ausferrite growth – the second step for ADI technology

The model of ausferrite growth

Ausferrite is a typical structure of austempered ductile iron (ADI). This is a mixture of ferrite and carbon supersaturated austenite with nodular graphite of distribution identical as in nodular graphite cast iron. Examined on a metallographic polished section, the ferrite in austenite matrix has a typical form of needles (acicular ferrite). However, taking into consideration the fact that the surface of a polished section is flat, the needles should be regarded rather as lamellae or disks. The correct ausferritic structure is free from the, typical of bainite, carbides.

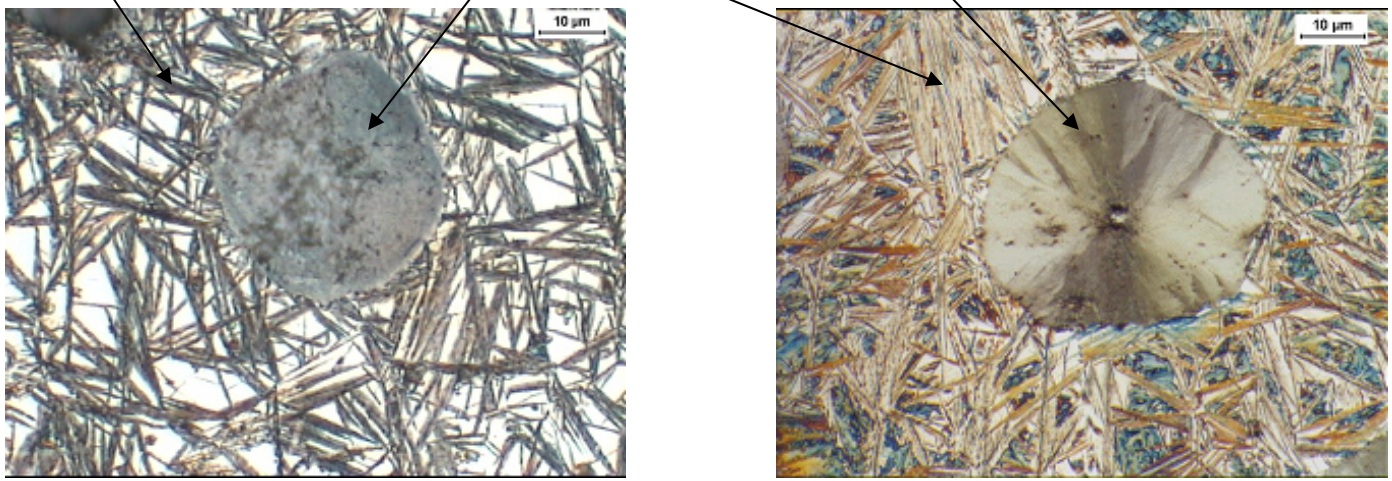

Fig. 2. Structure of ADI

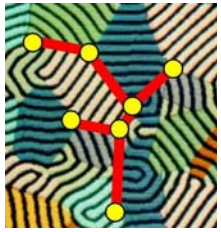

The model of ausferrite growth

As a base structure in ADI technology (after austenitizing) austenite with graphite nodules can be accepted, with carbon content in austenite amounting to 0.9 – 1.2 % carbon, according to the temperature of austenitizing (point C_0 at Fig. 3) . Rapid cooling of casting to austempering temperature (240 – 400ºC) changes the conditions of equilibrium, resulting in nucleation and growth of ferrite (with the concentration $C_{\alpha/\gamma}$) in austenite (with the concentration $C_{\gamma/\alpha}$ – Fig. 3*)* as an ausferrite.
It seems that the nomenclature "ausferrite" given to the structure constituents by Kovacs (AFS, 1994) is well justified although names like "bainite ferrite" or "bainite" instead of "ausferrite" are still in use.

The solution of the problem of modelling can be sought in a unidimensional system of Cartesian coordinates. The solution consists in quantitative approach to the problem of carbon diffusion in a system of ferrite – austenite, resulting from the change in thermodynamic conditions – from austenitisation temperature to austempering temperature. The obtained gradients of concentration make the mass diffusions and phase boundaries move, and specifically result in ferrite growth on account of austenite, coupled with changes in austenite saturation ratio, that is, in the formation of high-carbon reacted stable austenite.

The model of ausferrite growth

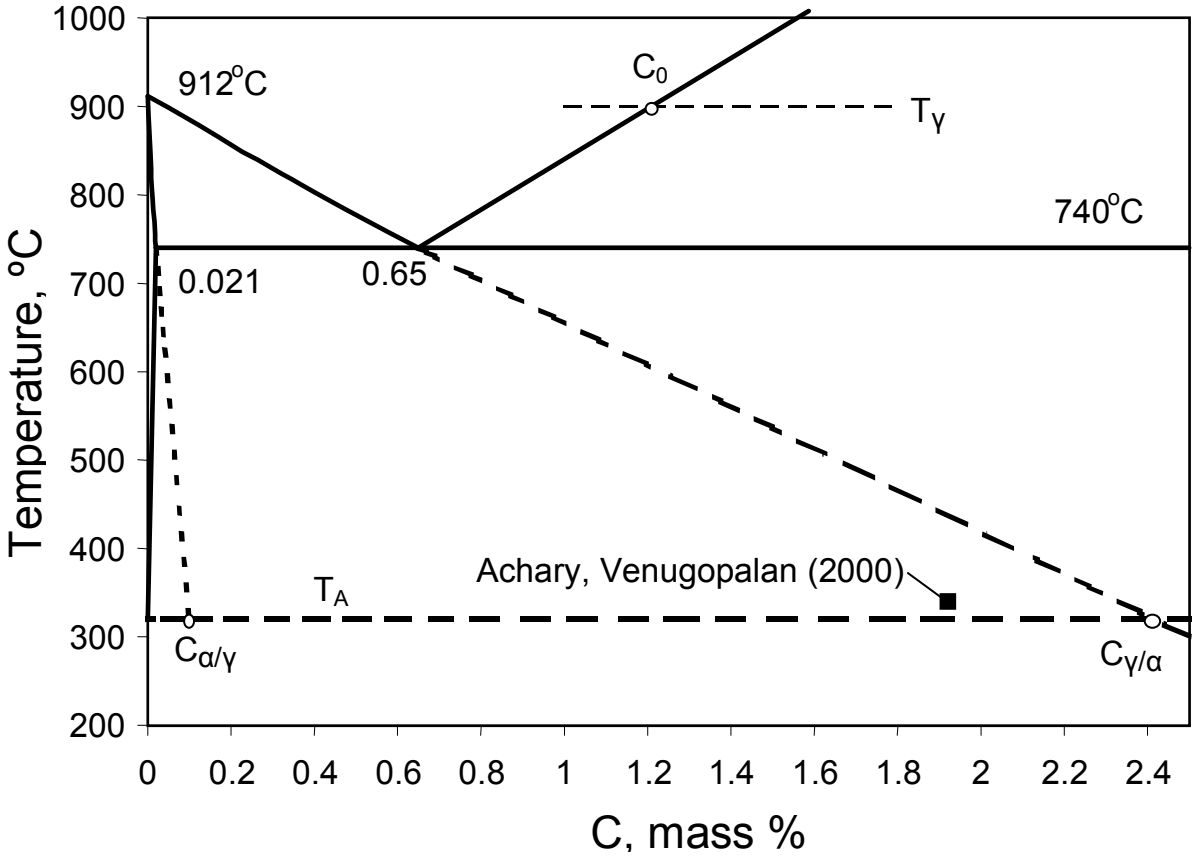

Fig. 3: The fragment of Fe-C equilibrium system. Point ■ - the experimental data.

The model of ausferrite growth - cont.

Figure 4 shows schematic representation of carbon concentration distribution during the growth of ferrite in austenite at an austempering temperature T_A. The respective symbols in Figure 4 correspond to a Fe-C phase diagram – Fig. 3.

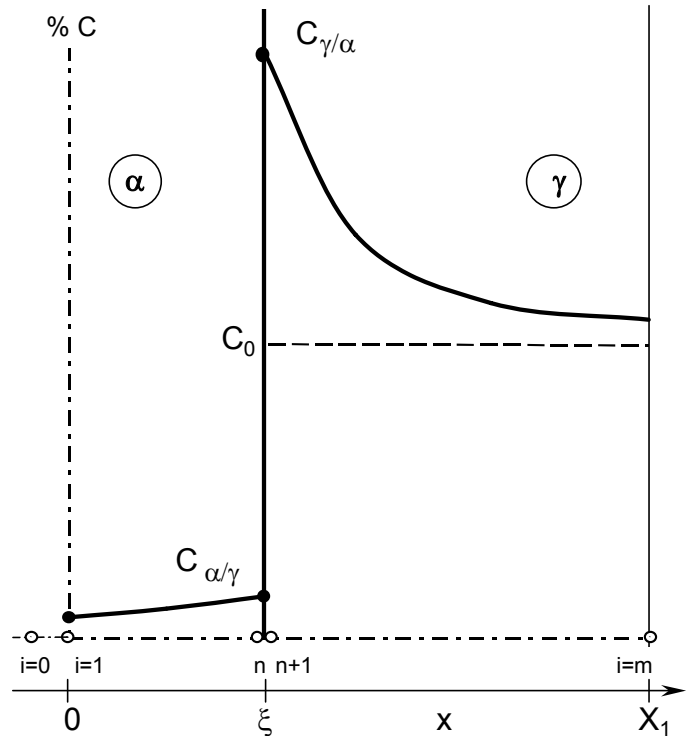

Fig. 4: The scheme of concentration

The model of ausferrite growth - cont.

The equations for the above model can be written for the α phase:

$$\frac{\partial C_\alpha}{\partial \tau} = D_\alpha \frac{\partial^2 C_\alpha}{\partial x^2} \qquad (1)$$

for the γ phase:

$$\frac{\partial C_\gamma}{\partial \tau} = D_\gamma \frac{\partial^2 C_\gamma}{\partial x^2} \qquad (2)$$

where C_α, C_γ – carbon concentration in ferrite and austenite;

D_α, D_γ – carbon diffusion coefficient for the given phase and at the given temperature of process (look at Fig. 5 on the rigth and Fig. 3, Lecture I)

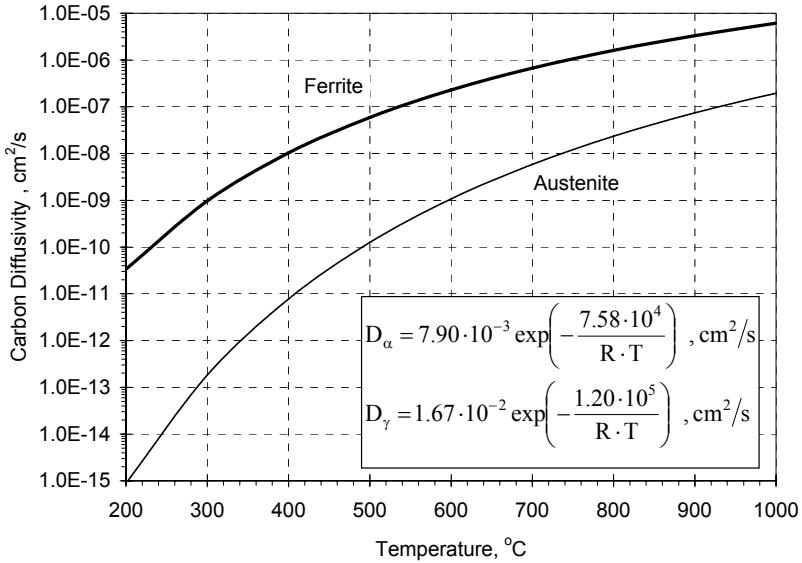

Fig. 5: Coefficient of carbon diffusion in austenite and ferrite

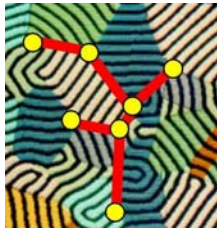

The model of ausferrite growth - cont.

Mass balance on the phase boundary (Fig. 2):

$$\left(C_{\alpha/\gamma}\,\rho_\alpha - C_{\gamma/\alpha}\,\rho_\gamma\right)\frac{d\xi}{d\tau} = D_\gamma\,\rho_\gamma\left(\frac{\partial C_\gamma}{\partial x}\right)_{x=\xi^+} - D_\alpha\,\rho_\alpha\left(\frac{\partial C_\alpha}{\partial x}\right)_{x=\xi^-} \qquad (3)$$

Boundary conditions:

for the α phase: $\dfrac{\partial C_\alpha}{\partial x} = 0, \quad x = 0$ and for the γ phase: $\dfrac{\partial C_\gamma}{\partial x} = 0, \quad x = X_1$

$$C = C_{\alpha/\gamma}, \quad x = \xi^+; \qquad C = C_{\gamma/\alpha}, \quad x = \xi^-$$

Initial conditions are given by the equilibrium system (Fig.3).

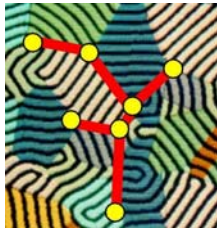

The model of ausferrite growth

Numerical solution

The rate of concentration variations according to equation (1) or (2) depends on the concentration gradient. Under the assumed boundary conditions, only a numerical solution seems to be possible.

If a model with constant number of differential elements within one single phase is assumed, the dimensions of these elements will change due to changes in thickness of this phase. The consequence will be that the, computed for a given point in the system, value of concentration of a constituent (reflected by the value of concentration in a given element) will depend not only on the concentration gradient but also on changes in the dimensions of a given element. The rate of changes in this concentration at a point inside the system, the position of which is a constant fraction of the changing phase thickness, can be expressed by a variable Muray-Landis lattice:

$$\frac{dC_i}{d\tau} = \frac{\partial C_i}{\partial x_i}\left(\frac{dx_i}{d\tau}\right) + \left(\frac{\partial C_i}{\partial \tau}\right) \qquad (4)$$

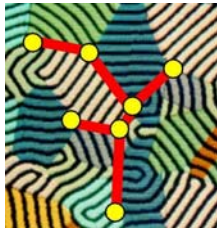

The model of ausferrite growth

Numerical solution

where: $\frac{\partial C_i}{\partial \tau}$ is determined by equations (1) or (2) and where the velocity of movement of an inside point „i” is functionally interrelated with the velocity of movement of the phase boundary:

$$\frac{dx_i}{d\tau} = \frac{x_i}{\xi}\frac{d\xi}{d\tau} \tag{5}$$

Combining (4) and (5) for the rate of phase con-cen-tra-tion changes at the inside point „i”, we obtain (for i=2,3...n-1 points across the a phase thickness):

$$\frac{dC_{i.\alpha}}{d\tau} = \frac{x_i}{\xi}\frac{\partial C_{\alpha.i}}{\partial x_i}\frac{d\xi}{d\tau} + \frac{\partial C_{i.\alpha}}{\partial \tau} \tag{6}$$

where: $\frac{d\xi}{d\tau}$ - the velocity of the phase boundary.

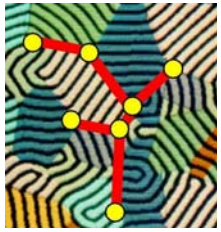

The model of ausferrite growth

Numerical solution

For the γ phase (for i = n+1 ... m-1 - Fig. 2):

$$\frac{dC_{i.\gamma}}{d\tau} = \frac{X_1 - x_i}{X_1 - \xi} \frac{\partial C_{\gamma.i}}{\partial x_i} \frac{d\xi}{d\tau} + \frac{\partial C_{i.\gamma}}{\partial \tau} \qquad (7)$$

For a phase boundary, equations (6) and (7) are related to the mass balance equation (3), the solution of which gives the velocity of movement of the phase boundary.

Transforming now equations (6) and (7) to the form of finite differences (under the assumption that the diffusivity is independent of concentration), we obtain (designations according to Fig. 4, for a network with variable dimensions of the differential elements):
for the phase α, at points $i \in (1, n-1)$

$$\frac{C_i^{k+1} - C_i^k}{\Delta\tau} = \frac{x_i}{\xi} \frac{C_{i+1}^k - C_{i-1}^k}{2\,\Delta x_1} \frac{d\xi}{d\tau}^{k+1} + \frac{D_\alpha}{\Delta x_1^2} \left(C_{i-1}^k - 2C_i^k + C_{i+1}^k \right) \qquad (8)$$

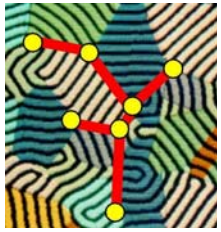

The model of ausferrite growth

Numerical solution

and for the phase γ, at points $i \in (n+2, m)$:

$$\frac{C_i^{k+1} - C_i^k}{\Delta\tau} = \frac{X_1 - x_i}{X_1 - \xi} \frac{C_{i+1}^k - C_{i-1}^k}{2\Delta x_2} \frac{d\xi^{k+1}}{d\tau} + \frac{D_\gamma}{\Delta x_2^2} \left(C_{i-1}^k - 2C_i^k + C_{i+1}^k\right) \quad (8)$$

(9)

where: k – the designations of the time step index,

Δx_1, Δx_2 – the size of differential elements in phases α and γ, respectively.

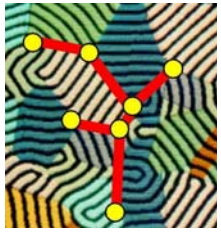

The model of ausferrite growth

Numerical solution

The velocity of the phase boundary movement u_ξ is determined from the mass balance equation (3) transformed to a differential form:

$$u_\xi = \frac{1}{C_{\alpha/\gamma} - C_{\gamma/\alpha}} \left[\frac{D_\gamma}{2\,\Delta x_2} \left(-C^k_{n+3} + 4C^k_{n+2} - 3C_{\gamma/\alpha} \right) - \frac{D_\alpha}{2\ \Delta x_1} \left(C^k_{n-2} - 4C^k_{n-1} + 3C_{\alpha/\gamma} \right) \right] \qquad (10)$$

where $u_\xi = \dfrac{\xi^{k+1} - \xi^k}{\Delta\tau}$

For elements lying on the system boundary, the derivative of the constitutent concentration equals zero, which enables us to write down the following:

$$C^{k+1}_0 = C^{k+1}_2; \qquad C^{k+1}_{m+1} = C^{k+1}_{m-1}$$

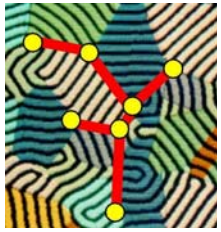

Ausferrite growth

Simulation

The above-mentioned mathematical model was used in development of a simulation program, the task of which was to trace the kinetics of ferrite growth in austenite under the conditions of austempering. The aim of the computations was to check model functioning for the assumed conditions of unequivocality. The main parameter was carbon diffusivity in austenite and ferrite which, varying in function of temperature, changes in a significant way the image of the process. The diffusivity was determined according to Figure 5.

Carbon diffusion coefficient for the ferrite and austenite (according to Fig. 5):

a) T=250ºC, $D_\alpha = 2.11 \times 10^{-10}$, $D_\gamma = 1.64 \times 10^{-14}$;

b) T=300ºC, $D_\alpha = 9.68 \times 10^{-10}$, $D_\gamma = 1.83 \times 10^{-13}$.

Ausferrite growth

Simulation

Figure 6 shows the kinetics at the ferrite-austenite phase boundary coupled with the field of diffusion for typical process duration, i.e. about 2 hours of austempering, and the diffusivity corresponding to a temperature of 250ºC (a) and 300ºC (b).

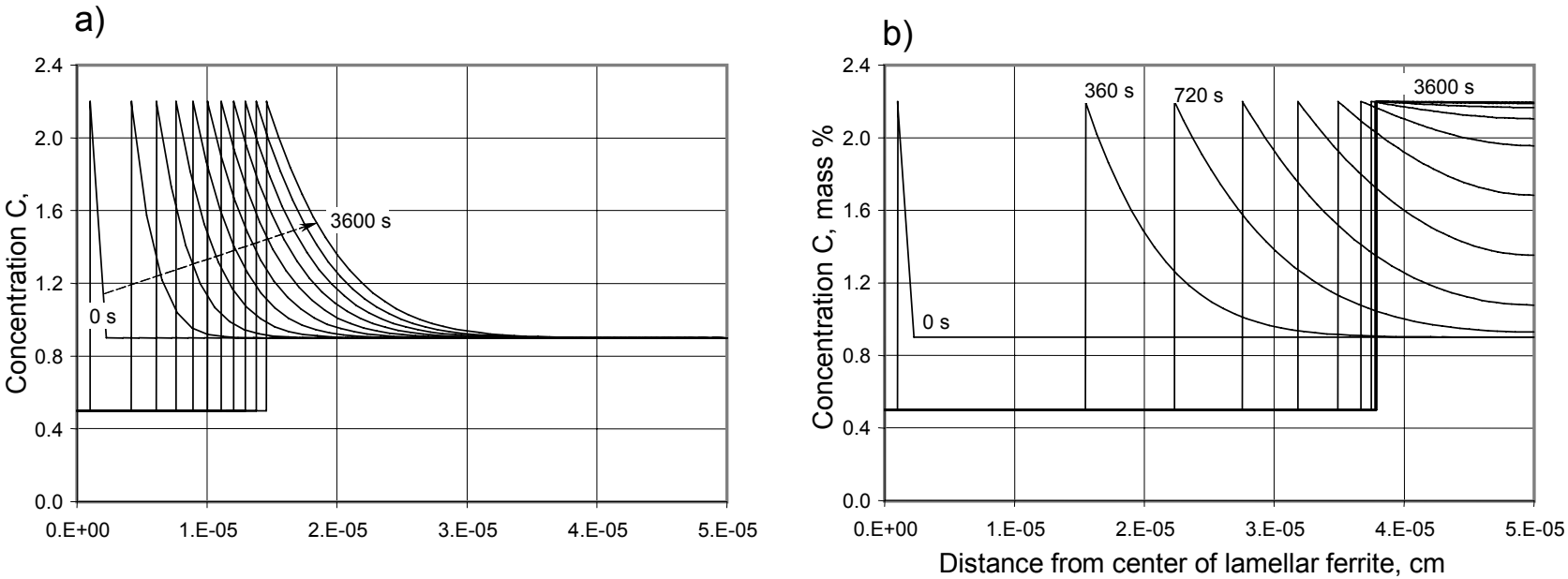

Fig. 6: Carbon concentration in ferrite and austenite as a function of time for tranformation temperature 250 (a) and 300^0C (b) - modelling.

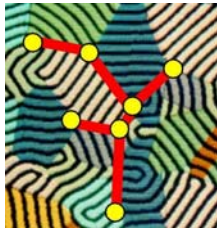

Ausferrite growth

Simulation

From the run of the curve illustrating the kinetics of concentration for temperature of transformation 250^0C (Fig. 6a) it follows that the process of ferrite lamella growth is proceeding very slowly; after the time of 3600 seconds the dimensions of the lamella are still very small and the growth has not been finished yet.

The same process for a diffusivity corresponding to a temperature of 300ºC (Fig. 6b) indicates finishing of the ferrite lamella growth after the time of about 1800 seconds.

Ausferrite growth

Experiments

Table 1: Composition of SGI for austempering

Content of elements [wt%]						
C	Mn	Si	P	S	Cr	Ni
3.45	0.21	2.32	0.069	0.012	0.04	1.68
Cu	Mg	Mo	Ti	Sn	Pb	
0.72	0.072	0.097	0.018	0.005	0.003	

Ausferrite growth

Nucleation of ferrite

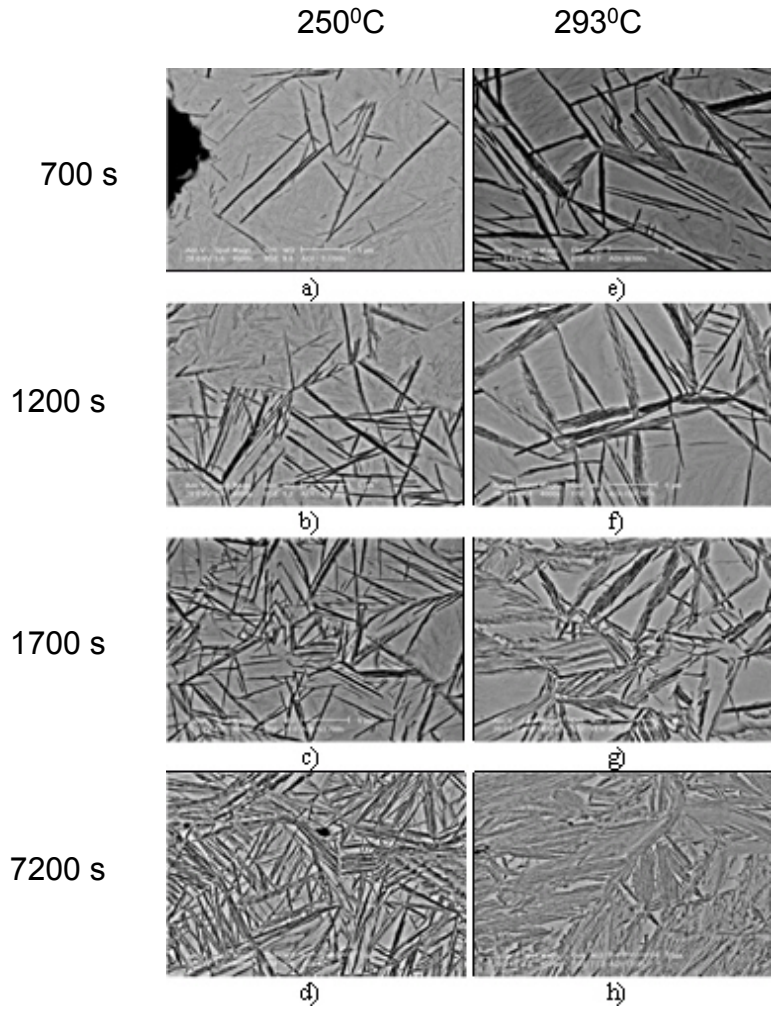

Fig. 7. Experimental morphology of ferrite plates in ausferritic structure ADI in time processing 700 (a, e), 1200 (b, f), 1700 (c, g) and 7200 seconds (d, h) and for the temperature processing 250ºC (a, b, c, d), 293ºC (e, f, g, h).

Ausferrite growth

Nucleation of ferrite

The kinetics of nucleation is shown in Figure 8, the experimental points (from Fig. 7) have been expressed by regression curves (Avrami type equation). The curves were used as input data in modelling. Using these functions of nucleation, the kinetics of ferrite volume growth in austenite (Fig. 9) and plate thickness of ferrite (Fig. 10) were computed for temperatures of 250 and 293ºC, and the results were compared with the data obtained by experiments.

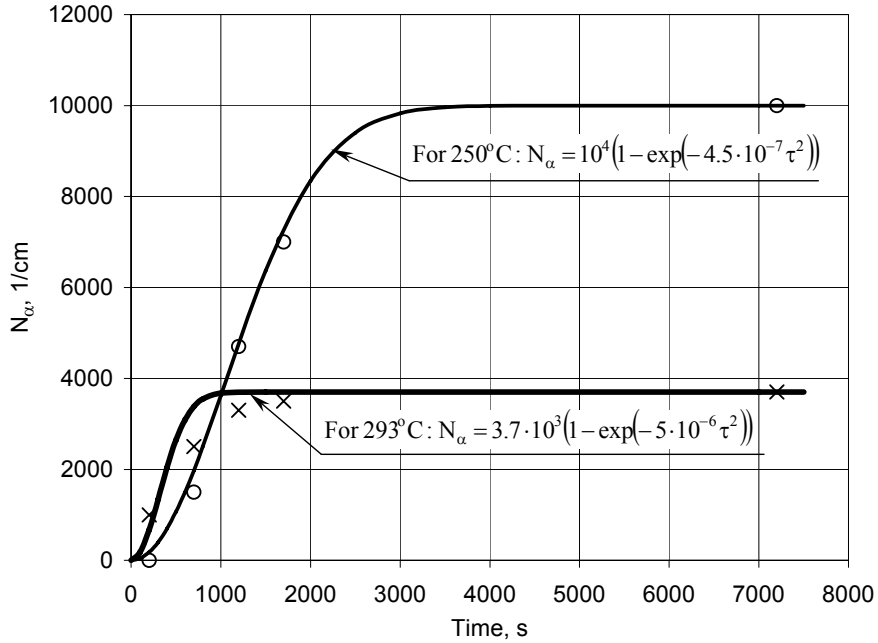

Fig. 8: The rate of ferrite nucleation (points: the experimental data)

From the performed simulation and data obtained in experiments it also follows that quite an important role in the kinetics of ausferrite formation is played by the nucleation of ferrite which is strongly dependent on both time and temperature of austempering.

Ausferrite growth

Modelling and experiments

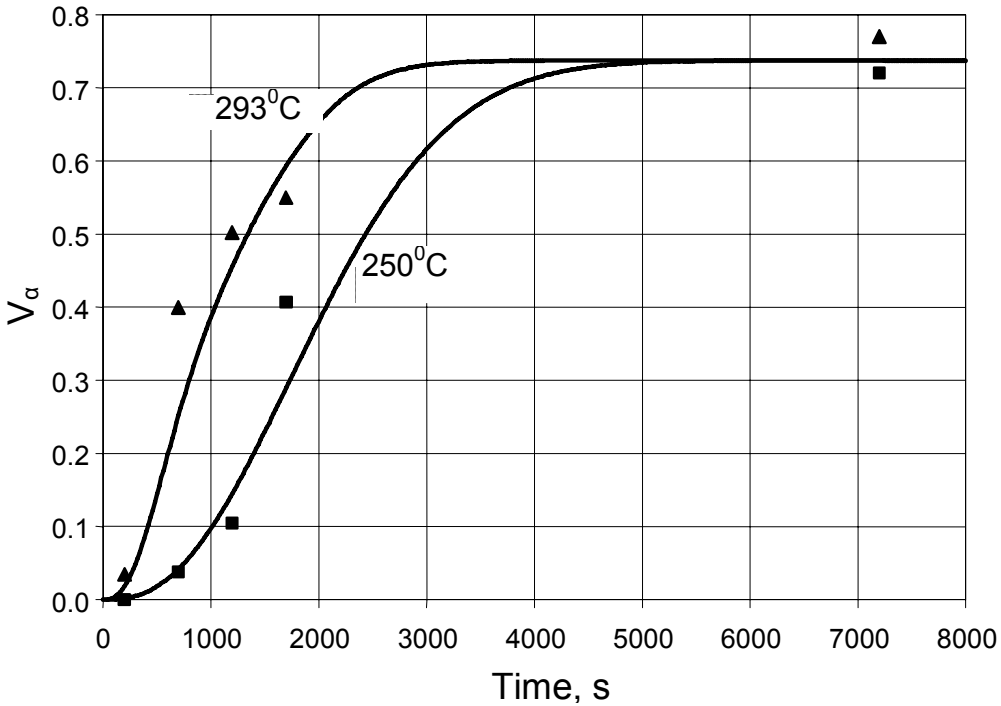

Fig. 9: The kinetics of ferrite volume (dimensionless) during austempering process (lines: simulation, points: the experimental data

Ausferrite growth

Experiments & modeling

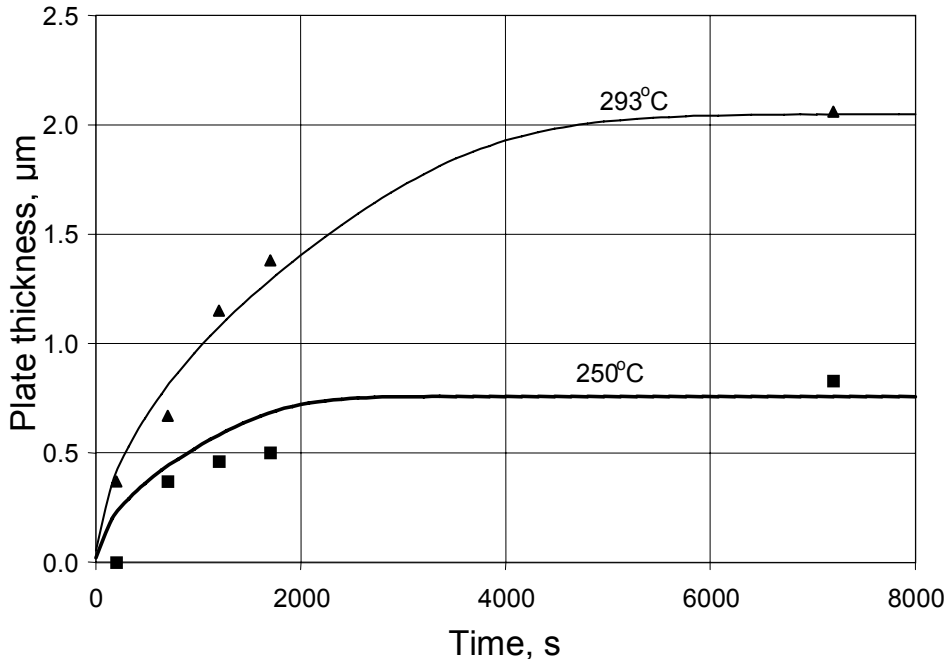

Fig. 10: The kinetics of ferrite plate growth during austempering process (lines: simulation, points: the experimental data)

The kinetics of ferrite volume and plate thickness during austempering process (Fig. 9 and 10) is strongly dependent on both time and temperature of austempering.

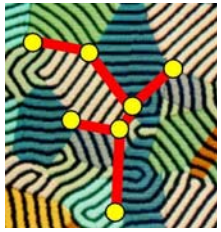

ADI - ausferrite growth

Summary

- Applying the developed model of the process and a program based on this model, a simulation of the kinetics of ferrite growth in austenite during austempering process was possible.
- The kinetics of ausferrite formation in ADI depends quite obviously on the austempering temperature, due to an effect exerted on the austenite diffusivity and austempering time.
- The short austempering time causes incomplete reaction of austenite, which is known to contribute to its transformation into martensite.